physics

MDPI

Communication

Finite-Size Effects of Casimir–van der Waals Forces in the Self-Assembly of Nanoparticles

Raul Esquivel-Sirvent

Instituto de Física, Universidad Nacional Autónomia de México, P.O. Box 20-364, Mexico City 01000, Mexico; raul@fisica.unam.mx

Abstract: Casimir–van der Waals forces are important in the self-assembly processes of nanoparticles. In this paper, using a hybrid approach based on Lifshitz theory of Casimir–van der Waals interactions and corrections due to the shape of the nanoparticles, it is shown that for non-spherical nanoparticles, the usual Hamaker approach overestimates the magnitude of the interaction. In particular, the study considers nanoplates of different thicknesses, nanocubes assembled with their faces parallel to each other, and tilted nanocubes, where the main interaction is between edges.

Keywords: self-assembly; Casimir force; van der Waals force; Hamaker constant; nanoparticles

1. Introduction

The self-assembly of nanoparticles has become an attractive area of research since it can be used to construct materials with novel properties by arranging nanoparticles of different geometries in arrays that mimic crystalline structures with a given periodicity [1]. Unlike usual crystals with an atom in each site, in self-assembled supracrystals, a nanoparticle is placed in the crystalline sites [2]. The assembly and bonding of the nanoparticles happen due to a combination of forces and, in many cases, ligands such as strands of nucleic acids [3]. Several physical properties can be modified in self-assembled systems, such as the optical response using plasmonic nanoparticles, as well as electrical and thermal conductivity properties, making self-assembly a practical way for building nanocomposites [4]. The potential use of nanocomposites as biosensors and nano-biomaterials has been studied [5], as well their therapeutic delivery of drugs at the nanoscale [6].

Self-assembly typically occurs in a solvent, such as water, and the interactions are described by the DLVO theory, named after Derjaguin, Landau, Verwey, and Overbeek. The DLVO theory includes the screened electrostatic interaction via the Poisson-Boltzman equation and the van der Waals interaction, assuming they are additive [7–10]. Depletion forces, that are attractive, due to the presence of micelles can also be present [11]The van der Waals force is usually calculated using the Hamaker approach, which assumes a pairwise summation [12]. Based on the fluctuation–dissipation theorem and Rytov's theory of fluctuating electrodynamics [13], Lifshitz [14,15] developed the theory of generalized van der Waals forces between macroscopic bodies. The Lifshitz equation for the Casimir–van der Waals interaction energy can be written as in the Hamaker's approach; however, now the Hamaker constant can be explicitly calculated if the dielectric functions of the particles and the surrounding media are known.

Of interest to the calculations presented in this paper is the equilibrium formation of colloidal Au nanoprisms. Young et al. synthesized and self-assembled triangular nanoprisms in a one-dimensional periodic array [16]. The periodicity of these lamellar superlattices depends on the solution's temperature and ionic strength. The equilibrium condition comes from the balance of the attractive van der Waals force, the repulsive electrostatic potential from the solution of the Poisson–Boltzmann equation, and the attractive depletion force that comes from the formation of micelles, since surfactants are added to

check for updates

Citation: Esquivel-Sirvent, R. Finite-Size Effects of Casimir–van der Waals Forces in the Self-Assembly of Nanoparticles. *Physics* **2023**, *5*, 322–330. https://doi.org/10.3390/physics5010024

Received: 2 February 2023
Revised: 4 March 2023
Accepted: 6 March 2023
Published: 21 March 2023

avoid aggregation. A similar work by Munkhbat et al. [17] designed tunable self-assembled Casimir microcavities made of parallel Au nano palettes and showed that only the electrostatic and Casimir–van der Waals interactions play a dominant role. Both above-described systems yield equilibrium periodic structures. The possibility of having optical cavities with a high-quality factor by combining the repulsive Casimir and buoyancy forces has also been considered [18]. A suitable choice of the dielectric functions of the plates and the media between them yields a repulsive force.

Finite-size effects due to the shape of the interacting bodies have been a challenge to the precise calculation of the Casimir–van der Waals force. Hamaker introduced [12] a pair-wise summation to calculate the interaction energy between two spheres, resulting in an expression that includes the energy of interaction multiplied by a factor that depends on the geometry of the objects. Other geometries have also been considered, such as the interaction between spheres and shells, as well as shells and walls [19]. Dantchev and Valchev presented [20] a surface integration approach generalizing the Derjaguin or proximity theorem approximation for the interaction between a three-dimensional object and a half-space. In particular, Dantchev and Valchev considered the case of spheres, cylinders, and the interaction of liposomes and lipid bilayers. The problem of extending the original theory of Hamaker is well described in an extensive review by Rusanov and Brodskaya [21], where they present the interaction of many systems of interest in colloidal science, such as spherical particles, wedges, and cylinders of different lengths.

Furthermore, we are interested in the self-assembly of polymer-grafted metal nanocubes into arrays of one-dimensional strings with well-defined interparticle orientations and tunable electromagnetic properties [22]. The nanocubes are assembled in two configurations: one considering the edge–to-edge interactions of the nanocubes, and the second one considering the face-to-face interactions. Unlike spherical nanoparticles characterized by one dipolar plasmonic resonance, cubes have several dipolar modes [23].

Since Lifshitz theory provides a more accurate description than the simple Hamaker approximation, a hybrid approach is preferred. In this paper, the interaction energy between two parallel surfaces is calculated using Lifshitz theory, adjusting for geometrical effects [24]. Within this approach and using the results of de Rocco and Hoover [25], we evaluate the Casimir–van der Waals interaction in several systems of interest in self-assembly.

2. Lifshitz Theory and the Hamaker Constant

Lifshitz theory considers two parallel slabs separated by a distance L and a temperature T. The plates have lateral dimensions that are much larger than L. The dielectric function of the plates is $\varepsilon(\omega)$ in a medium with a dielectric function $\varepsilon_{\mathrm{m}}(\omega)$. After making the rotation to imaginary frequencies $(\omega \to i\omega)$ and introducing the Matsubara frequencies $\zeta_n = 2\pi n K_B T/\hbar$, where K_B is Boltzmann constant, $\hbar$ is the reduced Planck's constant, and n is a natural number, the Casimir–van der Waals energy per unit area is written as [14,15,26]

$$\mathcal{E}(T,L) = \frac{K_B T}{2\pi} {\sum_{n=0}^{\infty}}' \int_0^{\infty} dQQ \ln[D_p(Q,\zeta_n,L) D_s(Q,\zeta_n,L)]. \quad (1)$$

The prime in the sum indicates that the $n = 0$ term has to be multiplied by $1/2$. The wave vector in the gap is $K_0 = (Q, k_0)$, with the z-component, $k_0 = \sqrt{\varepsilon_{\mathrm{m}}\zeta_n^2/c_0^2 + Q^2}$, where c_0 denotes the speed of light in vacuum. Within the material, the corresponding z component of the wave vector is $k = \sqrt{\varepsilon\zeta_n^2/c_0^2 + Q^2}$. These definitions of the normal components of the wave vectors are evaluated in the Matsubara frequencies. The function $D_\nu(Q,\zeta,L)$ is

$$D_\nu(Q,\zeta_n,L) = 1 - r_\nu^2 e^{-2k_0 L}, \quad (2)$$

where r_ν are the reflection coefficients of the plates for either $\nu = p$ or $\nu = s$ polarization. For clarity, it is important to notice that the reflection coefficients depend on the frequency

and parallel component of the wave vector Q through the definitions of k_0 and k, defined above. For a slab of thickness d, one has

$$r_\nu = \rho_\nu \frac{1 - e^{-2\delta}}{1 - \rho_\nu^2 e^{-2\delta}}, \tag{3}$$

where the phase δ is defined as $\delta = (d/c_0)\sqrt{\zeta_n^2(\varepsilon(i\zeta_n) - 1) + c_0^2 k_0}$, and the Fresnel coefficients ρ_ν are

$$\rho_s = \frac{k_0 - k}{k_0 + k}, \tag{4}$$

and

$$\rho_p = \frac{k - \varepsilon(i\zeta_n)k_0}{k + \varepsilon(i\zeta_n)k_0}. \tag{5}$$

In general, Equation (1) is correct for half-spaces, finite-width plates, layered systems [27], or nonlocal dielectric functions [28] provided that the appropriate reflection coefficients are calculated [29]. The only restriction is that Lifshitz theory assumes that the plate extension is infinite.

The interaction energy given by Equation (1) can be rewritten in the form of the Hamaker formula. Defining the variable $x = 2k_0 L$, the energy per unit area reads:

$$\mathcal{E}(T, L) = -\frac{A_H(T)}{12\pi L^2}, \tag{6}$$

where the Hamaker constant, $A_H(T)$, is

$$A_H(T) = -\frac{3kT}{2}{\sum_{n=0}^{\infty}}' \int_{x_0}^{\infty} dx\, x \ln[D_p(x, \zeta_n) D_s(x, \zeta_n)], \tag{7}$$

and the lower limit of integration is $x_0 = \zeta_n \sqrt{\varepsilon_m} L/c_0$.

For two equal plates facing each other of surface area S, the total energy is $E_H(L) = \mathcal{E}(L)S$.

3. Finite-Size Effects

When dealing with finite-size effects, the energy of interaction between the bodies can be, in general, written as $E(L, T) = A_H K(a, b, d)$, where $K(a, b, d)$ is a geometric correction that depends on the dimensions of the body indicated by a, b, d. However, A_H is calculated from Equation (7), which, as explained before, is for parallel plates strictly of infinite length or with dimensions much larger than the separation L. In what follows the following notation is used: E is the total energy between the bodies, and $\mathcal{E}$ is the energy density (see Equation (6)).

For the case of finite-size plates, the geometric factor was derived by De Rocco and Hoover [25]. For two parallel plates of size $a \times b$ and thickness c, the geometric factor is

$$\begin{aligned} K_{\mathrm{pl}}(x, a, b) = {} & \frac{1}{4} \ln\left(\frac{x^4 + x^2a^2 + x^2b^2 + a^2b^2}{x^4 + x^2a^2 + x^2b^2}\right) + \frac{x^2 - a^2}{4ax} \tan^{-1}\left(\frac{a}{x}\right) \\ & + \frac{x^2 - b^2}{4bx} \tan^{-1}\left(\frac{b}{x}\right) + \frac{x(a^2 + b^2)^{3/2}}{6a^2b^2} \tan^{-1}\left(\frac{x}{\sqrt{a^2 + b^2}}\right) \\ & + \left(\frac{1}{6x^2} + \frac{1}{6a^2}\right) b\sqrt{x^2 + a^2} \tan^{-1}\left(\frac{b}{\sqrt{a^2 + x^2)}}\right) \\ & + \left(\frac{1}{6x^2} + \frac{1}{6b^2}\right) a\sqrt{x^2 + a^2} \tan^{-1}\left(\frac{a}{\sqrt{b^2 + x^2}}\right). \end{aligned} \tag{8}$$

The variable x is a dummy variable that represents the position of the body where the geometric factor is evaluated. The corresponding interaction energy between the plates is

$$E(L,a,b,c) = -\frac{A_H}{\pi^2}[K_{\rm pl}(L+2c) - 2K_{\rm pl}(L+c) + K_{\rm pl}(L)]. \tag{9}$$

The other case of interest is the self-assembly of cubes (see Ref. [22]). Equations (8) and (9) are correct for two cubes with parallel faces, setting $a = b = c$. When the cubes are tilted and the interaction is edge-to-edge, the geometric factor of the interaction (denoted as K_{cb}) is

$$\begin{aligned} K(x,d,c)_{cb} = {} & \frac{1}{8}\ln\left(\frac{d^2+x^2}{c^2+d^2+x^2}\right) + \frac{1}{8}\left(\frac{x}{d}-\frac{d}{x}\right)\tan^{-1}\left(\frac{d}{x}\right) \\ & + \frac{(c^2+d^2)^{3/2}x}{12c^2d^2}\tan^{-1}\left(\frac{x}{\sqrt{d^2+c^2}}\right) \\ & + \frac{c\sqrt{d^2+x^2}}{12}\left(\frac{1}{d^2}+\frac{1}{x^2}\right)\tan^{-1}\left(\frac{c}{\sqrt{d^2+x^2}}\right) \\ & + \frac{d(c^2+x^2)^{1/2}}{12}\left(\frac{1}{c^2}+\frac{1}{x^2}\right)\tan^{-1}\left(\frac{d}{\sqrt{c^2+x^2}}\right), \end{aligned} \tag{10}$$

In this case, the separation L is between the edges of the cubes and $d = L/\sqrt{2}$, and the energy is

$$E(d,a,b,c) = -\frac{A_H}{\pi^2}(K_{cb}(d+2a,d,b,c) - 2K_{cb}(d+a,d,b,c) + K_{cb}(d,d,b,c)). \tag{11}$$

4. Results

To evaluate the finite-size effects, consider that the nanoparticles are made of Au with a dielectric function given by a Drude model: $\varepsilon(i\zeta_n) = 1 + w_p^2/(\zeta_n^2 + \zeta_n\gamma)$, where $w_p = 9$ eV and $\gamma = 0.02$ eV. The plates (and cubes) are surrounded by water. The dielectric function of the water used here is the data reported in Ref. [30] calculated along the rotated frequency space ($\omega \to i\zeta_n$).

To understand the effect of finite-size effects, let us compare the energy between the plates E_H and the energy predicted using Equation (9) and Equation (11). As was stated above, the energy for the plates E_H is given by $E_H = S\mathcal{E} = SA_H/12\pi L^2$. , where S is the surface of the plates. The value of the Hamaker constant in Refs. [16,17] was calculated assuming semi-infinite plates, which is $r_{s,p}$ in Equation (2)—the knownFresnel coefficients. Let us define the ratio $E_r = E(L;a,b,c)/E_H(L)$. If $E_r \sim 1$, then finite-size effects are not significant. Figure 1 shows E_r as a function of the separation for the case of parallel plates. The blue curve represents plates of size $a = b = 2000$ nm and thickness $c = 30$ nm, roughly the size reported in Ref. [17], and the red line corresponds to plates of size $a = b = 145$ nm and thickness $c = 7.5$ nm as in Ref. [16]. In both cases, one can observe that the Casimir–van der Waals interaction is underestimated when using Equation (6). As L decreases, the value of E_r increases, since $L \ll a, b$.

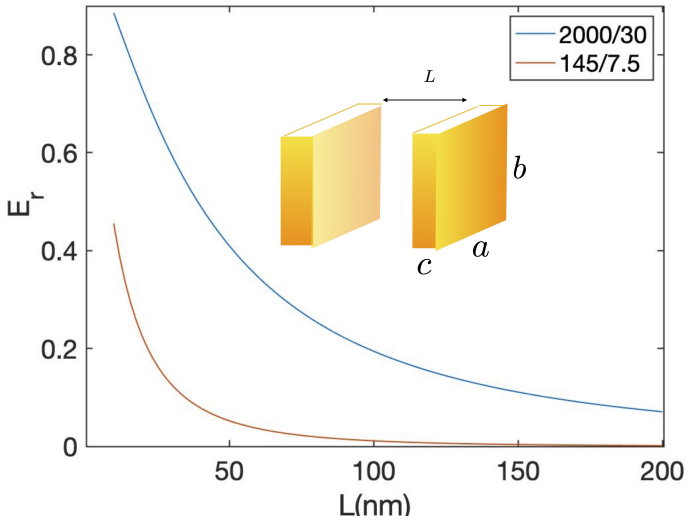

Figure 1. The energy ratio, E_r, for two sizes of square plates of size $a = b$ and thickness c. The lines correspond to the value a/c as indicated. The sizes correspond to those used in Refs. [16,17]. See text for details.

For completeness, Figure 2 shows how E_r changes with thickness c while the other dimensions are kept fixed ($a = b = 2000$ nm).

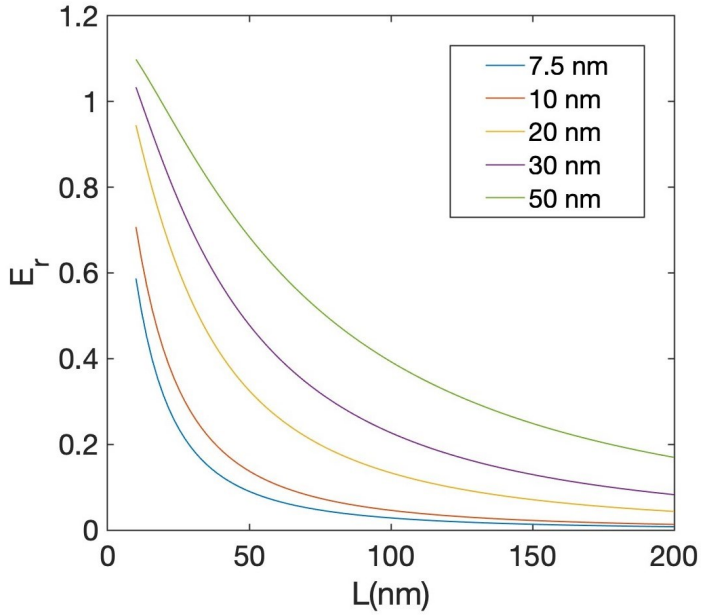

Figure 2. The variation of E_r as a function of the separation, L, of the two plates for different values of the thickness c of each as indicated, and $a = b = 2000$ nm. Even for large enough values of c, the energy ratio is less than unity.

At a fixed separation L, the dependence of E_r with the thickness, c, increases linearly for small values of c and levels off asymptotically to the value expected for half-spaces. Keeping the area of the plates constant and at two arbitrary separations of $L = 50$ nm and $L = 100$ nm, Figure 3 shows the variation with the thickness. Thus, one can quantify the correction needed for Equation (6).

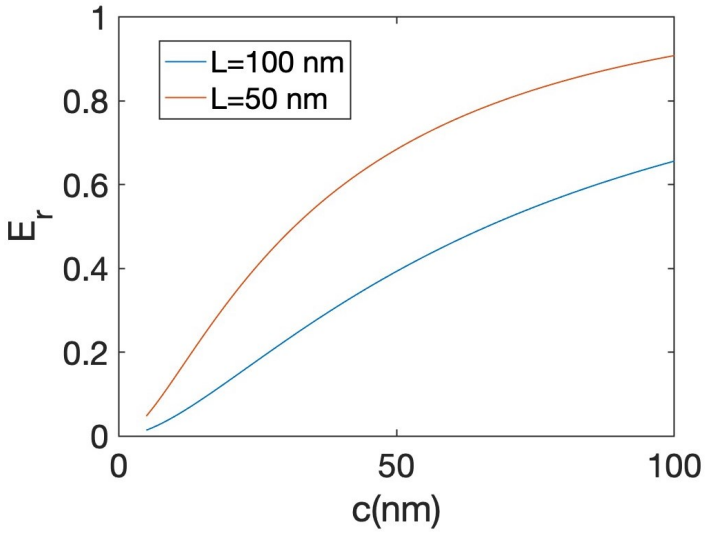

Figure 3. For two fixed separations between the plates, $L = 50$ nm and $L = 100$ nm, the ratio E_r increases with increasing the value of the thickness c, leveling-off asymptotically to the value expected for half-spaces. The dimensions of the plate are $a = b = 2000$ nm.

The interaction energy E_r for cubes is presented in Figure 4. The face–face and edge–edge interactions are considered with edge lengths of $a = b = c = 80$ nm as reported in Ref. [22]. The face–face interaction is just a particular case of parallel plates with $a = b = c$, and the behavior is the same. As L decreases, the ratio a/L increases, and E_r increases. For all separations L, since $E_r < 1$, one can see that using Equation (6) overestimates the interaction. The ratio E_r is calculated using Equation (11) for the edge–edge interaction. The behavior of E_r is different from the other cases. For the tilted cubes, the behavior is different, and the interaction increases with increasing separation until it reaches a maxima. To further understand this behavior, E_r is plotted Figure 5 for the edge–edge interaction for cubes of different sizes. The behavior of the curves is the same for different sizes except that, depending on the size of the cube, there are different values of the maxima,but it occurs when the separation between the edges is the same as the size of the cube $L = c$. It should also be noted that the maximum value attained by E_r is independent of the size of the cube. Whether this is an artifact of the Hamaker approach or due to the singularity of having the interaction between two edges is an issue that needs further exploration.

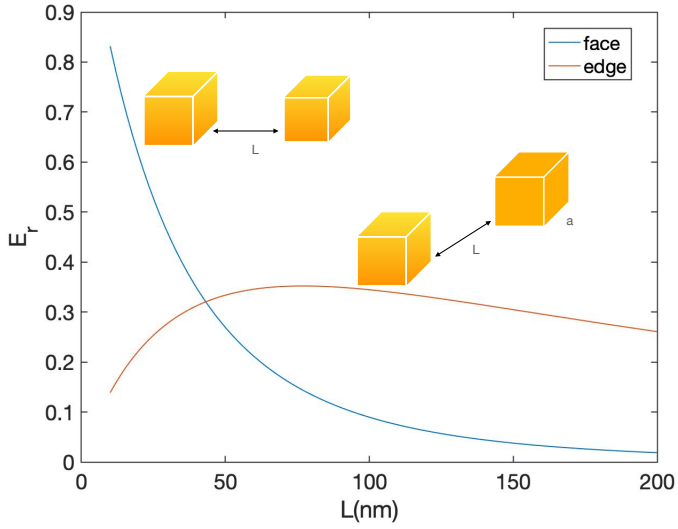

Figure 4. Energy ratio, E_r between two cubes facing each other and for two tilted cubes, as a function of the separation L. The nanocubes have dimensions $a = b = c = 80$ nm.

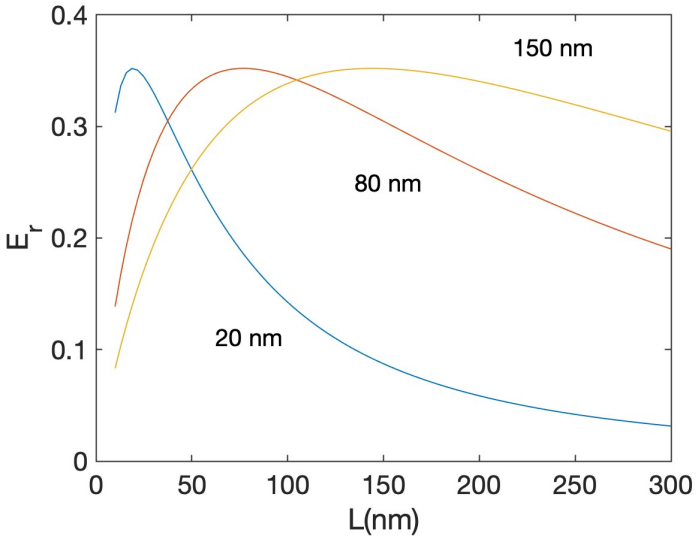

Figure 5. Energy ratio, E_r, between two tilted nanocubes of different sizes. The sizes considered are 20 nm (blue line), 80 nm (red line), and 150 nm (orange line). The maximum in each curve happens when the separation equals the size of the cube.

5. Discussion

The results presented in this study assumed that the surrounding medium was water. No effect of electrolytes that screen the van der Waals interaction [31,32] was considered. The screening will change the magnitude of the interaction energy. The dielectric function of the nanoparticle is assumed to be that of bulk Au. In the case of small metallic nanoparticles, the damping has to be corrected to consider the change in the electronmean-free path. For silver, this correction implies a change in the Hamaker constant of 138% nanoparticles [33].

In the case of plates and nanoparticles, there is another effect that has not been considered: spatial dispersion or nonlocal effects. For plates whose thickness is less than the electron mean-free path, or with nanoparticles with an average size smaller than the mean-free path, the dependence of the dielectric function with the wave vector has to be taken into account. As shown in Ref. [34], introducing spatial dispersion affects the Hamaker constant's value at short separations. The difference in the Hamaker constant between the local and nonlocal cases can be as large as two orders of magnitude. Nonlocal effects become relevant when the size of the bodies is of the order of magnitude of the skin depth. For Au (depending on the frequency), the skin depth is ∼40 nm. Thus, the nanoplates used for self-assembly in the literature [16,17] fall in the range of thickness where spatial dispersion has to be taken into account.

6. Conclusions

The ability to synthesize nanoparticles of different shapes and use them in self-assembly requires understanding all the interactions, particularly the Casimir–van der Waals interaction. The simplified approach not taking into account the shape overestimates the force. The use of Equations (6) and (7) is not the only procedure available in the literature for estimating the Casimir–van der Waals interaction. Numerical simulations for arbitrary 3D objects have been reported earlier [35] but require more computer-intensive calculations. The procedure presented in this paper can be considered a first approach to estimating the influence of the geometry for the case of nanoplates and nanocubes. The interaction energy obtained, considering finite-size effects, is smaller than that predicted by the conventional Hamaker approach. Geometric effects and other considerations, such as spatial dispersion, should provide a better prediction of the Casimir–van der Waals interaction for an accurate design of self-assembled structures.

Funding: This research received no external funding.

Data Availability Statement: Not applicable.

Acknowledgments: The author thanks Shunashi G. Castillo-López for helpful discussions and comments to the manuscript.

Conflicts of Interest: The author declares no conflict of interest.

References

1. Jones, M.R.; Macfarlane, R.J.; Lee, B.; Zhang, J.; Young, K.L.; Senesi, A.J.; Mirkin, C.A. DNA-nanoparticle superlattices formed from anisotropic building blocks. *Nat. Mat.* **2010**, *9*, 913–917. [CrossRef] [PubMed]
2. Macfarlane, R.J.; Lee, B.; Jones, M.R.; Harris, N.; Schatz, G.C.; Mirkin, C.A. Nanoparticle superlattice engineering with DNA. In *Spherical Nucleic Acids. Volume 2*; Mirkin, C.A., Ed.; Jenny Stanford Publishing: New York, NY, USA, 2020; Chapter 23.
3. Wu, C.; Han, D.; Chen, T.; Peng, L.; Zhu, G.; You, M.; Qiu, L.; Sefah, K.; Zhang, X.; Tan, W. Building a multifunctional aptamer-based DNA nanoassembly for targeted cancer therapy. *J. Am. Chem. Soc.* **2013**, *135*, 18644–18650. [CrossRef] [PubMed]
4. Genix, A.C.; Oberdisse, J. Nanoparticle self-assembly: From interactions in suspension to polymer nanocomposites. *Soft Matt.* **2018**, *14*, 5161–5179. [CrossRef] [PubMed]
5. Mendes, A.C.; Baran, E.T.; Reis, R.L.; Azevedo, H.S. Self-assembly in nature: Using the principles of nature to create complex nanobiomaterials. *WIREs (Wiley Interdiscip. Rev.) Nanomed. Nanobiotechnol.* **2013**, *5*, 582–612. [CrossRef] [PubMed]
6. Yadav, S.; Sharma, A.K.; Kumar, P. Nanoscale self-assembly for therapeutic delivery. *Front. Bioeng. Biotechnol.* **2020**, *8*, 127. [CrossRef] [PubMed]
7. Verwey, E.J.W. Theory of the stability of lyophobic colloids. *J. Phys. Chem.* **1947**, *51*, 631–636. [CrossRef]
8. Birdi, K.S. *Handbook of Surface and Colloid Chemistry*; CRC Press/Taylor & Francis Group: Boca Raton, FL, USA, 2008. [CrossRef]
9. Jose, N.A.; Zeng, H.C.; Lapkin, A.A. Hydrodynamic assembly of two-dimensional layered double hydroxide nanostructures. *Nat. Comm.* **2018**, *9*, 1–12. [CrossRef]
10. French, R.H.; Parsegian, V.A.; Podgornik, R.; Rajter, R.F.; Jagota, A.; Luo, J.; Asthagiri, D.; Chaudhury, M.K.; Chiang, Y.M.; Granick, S.; et al. Long range interactions in nanoscale science. *Rev. Mod. Phys.* **2010**, *82*, 1887–1944. [CrossRef]
11. Trokhymchuk, A.; Henderson, D. Depletion forces in bulk and in confined domains: From Asakura–Oosawa to recent statistical physics advances. *Curr. Opin. Colloid Interface Sci.* **2015**, *20*, 32–38. [CrossRef]
12. Hamaker, H.C. The London—van der Waals attraction between spherical particles. *Physica* **1937**, *4*, 1058–1072. [CrossRef]
13. Vinogradov, E.A.; Dorofeev, I.A. Thermally stimulated electromagnetic fields of solids. *Phys.-Usp.* **2009**, *52*, 425–459. [CrossRef]
14. Lifshitz, E.M. The theory of molecular attractive forces between solids. *Sov. Phys. JETP* **1956**, *2*, 73–83. Available onine: http://jetp.ras.ru/cgi-bin/e/index/e/2/1/p73?a=list (accessed on 1 March 2023).
15. Dzyaloshinskii, I.E.; Lifshitz, E.M.; Pitaevskii, L.P. General theory of Van der Waals' forces. *Sov. Phys. Usp.* **1961**, *4*, 153–176. [CrossRef]
16. Young, K.L.; Jones, M.R.; Zhang, J.; Macfarlane, R.J.; Esquivel-Sirvent, R.; Nap, R.J.; Wu, J.; Schatz, G.C.; Lee, B.; Mirkin, C.A. Assembly of reconfigurable one-dimensional colloidal superlattices due to a synergy of fundamental nanoscale forces. *Proc. Nat. Acad. Sci. USA* **2012**, *109*, 2240–2245. [CrossRef]
17. Munkhbat, B.; Canales, A.; Küçüköz, B.; Baranov, D.G.; Shegai, T.O. Tunable self-assembled Casimir microcavities and polaritons. *Nature* **2021**, *597*, 214–219. [CrossRef] [PubMed]
18. Esteso, V.; Carretero-Palacios, S.; Míguez, H. Casimir–Lifshitz force based optical resonators. *J. Phys. Chem. Lett.* **2019**, *10*, 5856–5860. [CrossRef]
19. Tadmor, R. The London-van der Waals interaction energy between objects of various geometries. *J. Phys. Cond. Matt.* **2001**, *13*, L195–L202. [CrossRef]
20. Dantchev, D.; Valchev, G. Surface integration approach: A new technique for evaluating geometry dependent forces between objects of various geometry and a plate. *J. Colloid Interface Sci.* **2012**, *372*, 148–163. [CrossRef]
21. Rusanov, A.I.; Brodskaya, E.N. Dispersion forces in nanoscience. *Russ. Chem. Rev.* **2019**, *88*, 837–874. [CrossRef]
22. Gao, B.; Arya, G.; Tao, A.R. Self-orienting nanocubes for the assembly of plasmonic nanojunctions. *Nat. Nanotech.* **2012**, *7*, 433–437. [CrossRef]
23. Langbein, D. Normal modes at small cubes and rectangular particles. *J. Phys. A Math. Gen.* **1976**, *9*, 627–644. [CrossRef]
24. Parsegian, V.A. *Van der Waals Forces. A Handbook for Biologists, Chemists, Engineers, and Physicists*; Cambridge University Press: New York, NY, USA, 2005. [CrossRef]
25. De Rocco, A.G.; Hoover, W.G. On the interaction of colloidal particles. *Proc. Nat. Acad. Sci. USA* **1960**, *46*, 1057–1065. [CrossRef] [PubMed]
26. French, R.H. Origins and applications of London dispersion forces and Hamaker constants in ceramics. *J. Am. Ceram. Soc.* **2000**, *83*, 2117–2146. [CrossRef]
27. Pinto, F. Computational considerations in the calculation of the Casimir force between multilayered systems. *Int. J. Mod. Phys. A* **2004**, *19*, 4069–4084. [CrossRef]
28. Esquivel-Sirvent, R.; Svetovoy, V. Nonlocal thin films in calculations of the Casimir force. *Phys. Rev.* **2005**, *72*, 045443. [CrossRef]

29. Mochán, W.L.; Villarreal, C.; Esquivel-Sirvent, R. On Casimir forces for media with arbitrary dielectric properties. *Rev. Mex. Fis.* **2002**, *48*, 339–342. Available online: https://www.scielo.org.mx/scielo.php?script=sci_arttext&pid=S0035-001X2002000400010 (accessed on 1 March 2023).
30. Roth, C.M.; Lenhoff, A.M. Improved parametric representation of water dielectric data for Lifshitz theory calculations. *J. Colloid Interface Sci.* **1996**, *179*, 637–639. [CrossRef]
31. Fiedler, J.; Walter, M.; Buhmann, S.Y. Effective screening of medium-assisted van der Waals interactions between embedded particles. *J. Chem. Phys.* **2021**, *154*, 104102. [CrossRef]
32. Nunes, R.O.; Spreng, B.; de Melo e Souza, R.; Ingold, G.L.; Maia Neto, P.A.; Rosa, F.S.S. The Casimir interaction between spheres immersed in electrolytes. *Universe* **2021**, *7*, 156. [CrossRef]
33. Pinchuk, A.O. Size-dependent Hamaker constant for silver nanoparticles. *J. Phys. Chem. C* **2012**, *116*, 20099–20102. [CrossRef]
34. Esquivel-Sirvent, R.; Schatz, G.C. Spatial nonlocality in the calculation of Hamaker coefficients. *J. Phys. Chem. C* **2012**, *116*, 420–424. [CrossRef]
35. Reid, M.H.; Rodriguez, A.W.; White, J.; Johnson, S.G. Efficient computation of Casimir interactions between arbitrary 3D objects. *Phys. Rev. Lett.* **2009**, *103*, 040401. [CrossRef] [PubMed]